Original Article

Altered functional connectivity density and structural covariance networks in women with premenstrual syndrome

Chengxiang Liu[1,2,3#], Gaoxiong Duan[4#], Shuming Zhang[1,2,3], Yichen Wei[4], Lingyan Liang[4], Bowen Geng[1,2,3], Ruiqing Piao[1,2,3], Ke Xu[1,2,3], Pengyu Li[1,2,3], Xiao Zeng[1,2,3], Demao Deng[4], Peng Liu[1,2,3]^

[1]Life Science Research Center, School of Life Science and Technology, Xidian University, Xi'an, China; [2]Engineering Research Center of Molecular and Neuro Imaging Ministry of Education, School of Life Science and Technology, Xidian University, Xi'an, China; [3]Xi'an Key Laboratory of Intelligent Sensing and Regulation of Trans-Scale Life Information, School of Life Science and Technology, Xidian University, Xi'an, China; [4]Department of Radiology, the People's Hospital of Guangxi Zhuang Autonomous Region, Nanning, China

Contributions: (I) Conception and design: P Liu; (II) Administrative support: P Liu; (III) Provision of study materials or patients: G Duan; (IV) Collection and assembly of data: C Liu; (V) Data analysis and interpretation: C Liu; (VI) Manuscript writing: All authors; (VII) Final approval of manuscript: All authors.

[#]The authors contributed equally to this work.

Correspondence to: Peng Liu, PhD. Life Sciences Research Center, School of Life Science and Technology, Xidian University, Xi'an 710071, China. Email: liupengphd@gmail.com; Demao Deng, MD. Department of Radiology, the People's Hospital of Guangxi Zhuang Autonomous Region, Nanning 530021, China. Email: demaodeng@163.com.

Background: Premenstrual syndrome (PMS) is a menstrual-related disorder, characterized by physical, emotional, behavioral and cognitive symptoms. However, the neuropathological mechanisms of PMS remain unclear. This study aimed to investigate the frequency-specific functional connectivity density (FCD) and structural covariance in PMS.

Methods: Functional and T1-weighted structural data were obtained from 35 PMS patients and 36 healthy controls (HCs). This study was a cross-sectional and prospective design. The local/long-range FCD (LFCD/LRFCD) across slow-4 (0.027–0.073 Hz) and slow-5 (0.01–0.027 Hz) bands were computed, and two-way analysis of variance (ANOVA) was performed to ascertain the main effects of group and interaction effects between group and frequency band. Receiver operating characteristic (ROC) curve was performed to investigate reliable biomarkers for identifying PMS from HCs. Based on the ROC results, characterized the changes of whole-brain structural covariance patterns of striatum subregions in two groups. Correlation analysis was applied to examine relationships between the clinical symptoms and abnormal brain regions.

Results: Compared with HCs, PMS patients exhibited: (I) aberrant functional communication in the middle cingulate cortex and precentral gyrus; (II) significant frequency band-by-group interaction effects of the striatum, thalamus and orbitofrontal cortex; (III) the better classification ability of the LFCD in the striatum in ROC analysis (slow-5); (IV) decreased gray matter volumes in the caudate subregions and decreased structural associations of between the caudate subregions and frontal cortex; (V) the LFCD value in thalamus were significantly negatively correlated with the sleep problems (slow-5).

Conclusions: Based on multi-modal magnetic resonance imaging (MRI) analysis, this study might imply the aberrant emotional regulation and cognitive function related to menstrual cycle in PMS and improve our understanding of the pathophysiologic mechanism in PMS from novel perspective.

Keywords: Magnetic resonance imaging (MRI); premenstrual syndrome (PMS); frequency-specific; functional

^ ORCID: 0000-0001-6965-8001.

connectivity density (FCD); structural covariance

Submitted May 20, 2022. Accepted for publication Nov 21, 2022. Published online Jan 02, 2023.
doi: 10.21037/qims-22-506
View this article at: https://dx.doi.org/10.21037/qims-22-506

Introduction

Premenstrual syndrome (PMS) is a menstrual-related disorder, which refers to a set of cyclical and relapsing physical, emotional, behavioral and cognitive symptoms that regularly recur during the late luteal phase of each menstrual cycle. Peaking within the week preceding menses and improving or relieving after the onset of menses (1,2). PMS occurs in 30–40% of reproductive-age females (1). The women who suffer from PMS are often affected by negative emotions such as anxiety, depression and irritability (3,4). Besides, it affects women's quality of life, work, family, relationships, productivity, social activity (5). Given the high proportion of women experiencing PMS, its pathophysiologic mechanism has attracted extensive attention among researchers in recent years. However, the exact pathophysiology mechanisms of PMS remain unclear.

Recently, altered hippocampus-related intrinsic connectivity were detected in PMS, such as the medial prefrontal cortex (MPFC), precentral gyrus (PreCG) and orbitofrontal cortex (OFC) (6). Independent component analysis (ICA) demonstrated the abnormalities of the middle frontal cortex (MFC)-related and PreCG-related intrinsic connectivity in PMS (7). In a graph-theoretical based study, Liu *et al.* demonstrated that PMS had abnormal node properties in several regions, including the PreCG, OFC, putamen, pallidum and thalamus (8). Moreover, structural magnetic resonance imaging (sMRI) studies have demonstrated that altered subcortical volumes in the thalamus and pallidum in PMS patients compared with healthy controls (HCs) (9), and abnormal thalamus-related covariance patterns mainly associated with the PreCG and putamen in PMS patients (10). To some extent, these studies may provide support for the abnormal brain neural mechanisms of PMS patients. However, the changed pattern of functional connectivity (FC) and structural are still not fully understood in PMS.

Although the intriguing findings in PMS, previous FC, ICA and graph theory studies limited the potential to fully assess the functional properties of brain networks. As a combination of voxel-wise FC and graph theory analyses, functional connectivity density (FCD) mapping is a powerful approach for depicting whole-brain FC through the calculation of local FCD (LFCD) and long-range FCD (LRFCD) (11,12). The efficient and well-organized functioning of the human brain depends upon local and remote connections (13). Previous studies have evidenced that FCD is well suited for the systematic study of FC abnormalities in the brain (11,12,14), the identification of specific pathophysiological functional signatures, and the revelation of the neural mechanisms underlying dysfunctions in various psychiatric disorders (15,16). These researches infer the promise of FCD as a powerful method for PMS-related investigations. The low-frequency oscillations amplitudes in different frequency bands are thought to reflect distinct properties and physiological functions of brain activity (17,18). Specifically, the frequency spectrum was decomposed into five distinct frequency bands, including slow-6 (0–0.01 Hz), slow-5 (0.01–0.027 Hz), slow-4 (0.027–0.073 Hz), slow-3 (0.073–0.198 Hz), and slow-2 (0.198–0.25 Hz). It has been shown that the oscillation amplitudes of the slow-4 and slow-5 bands occur in the gray matter (GM) and are conducive to identify correlations of functional processing and diseases. In accordance with previous studies, slow-6, slow-3, and slow-2 oscillations were discarded (18,19). By examining the FCD in the slow-4 and slow-5 bands, frequency-specific alterations of brain connectivity were determined in psychiatric disorders including early-onset schizophrenia (15), bipolar disorder depression (16). Moreover, previous studies have identified that the higher amplitude of low-frequency fluctuations/fractional amplitude of low-frequency fluctuations values including the basal ganglia and temporal regions in the slow-5 band compared to the slow-4 band in amnestic mild cognitive impairment (20) and Alzheimer's disease dementia (21). These previous studies have proposed that the pattern of intrinsic brain activity is sensitive to specific frequency bands (i.e., slow-5). Structural covariance, providing an effective way to investigate the covariance pattern of GM morphological properties of a

region with the other voxels or regions in the brain (22). A consistency among structural covariance networks, anatomical connectivity networks and FC networks was reveled in previous studies, which provides powerful support for applying structural covariance method to assess network integrity in various neuropsychiatric disorders (23,24).

Thereby, we combined frequency-specific FCD and structural covariance analysis to explore abnormal FC and covariance patterns in PMS patients, which may provide potential value for further understanding the pathophysiology mechanisms of PMS patients. Here, we hypothesized that (I) the significant different connectivity patterns would be demonstrated between PMS patients and HCs; (II) the interaction effects between groups and frequency bands would be ascertained; (III) the altered structural covariance patterns would be demonstrated between PMS patients and HCs; (IV) the possible relationships between neuroimaging findings might be correlated with clinical symptoms among PMS patients. We present the following article in accordance with STROBE reporting checklist (available at https://qims.amegroups.com/article/view/10.21037/qims-22-506/rc).

Methods

Ethical statement and experimental paradigm

This study was a cross-sectional and prospective design. The study was conducted in accordance with the Declaration of Helsinki (as revised by 2013) (25). The study was approved by the Medicine Ethics Committee of First Affiliated Hospital, Guangxi University of Chinese Medicine (No. 2018-037-02). Each participant was instructed to the whole experiment procedures and signed informed consent forms before experimentation. This study was registered in the Chinese Clinical Trial Registry and available at http://www.chictr.org.cn as registration number was ChiCTR1900020642.

In accordance with the females' physical characteristics and hormone level, all the magnetic resonance imaging (MRI) scanning were executed in the late-luteal phase, ranging from 1 to 7 days prior to menstruation. In order to exclude organic diseases and verify menstrual cycle stage, gynecological examination and B-ultrasonic wave were adopted for each participant before this study. To obtain the relatively stable and low level of endogenous cortisol and estradiol, all of the MRI scan tests were performed between 20:00 and 22:00 pm (26).

Participants

The daily rating of severity of problems (DRSP) is considered as a reliable, valid and sensitive tool for prospective assessment of severity of symptoms and impairment at various phases of menstrual cycle. The DRSP consists of 21 separate items grouped within 11 domains describing emotional, physical, cognitive and behavioral premenstrual symptoms and 3 specific items of impairment in functioning caused by the symptoms (27). In order to quantify premenstrual symptoms, each participant underwent two months of prospective screening and was asked to complete a DRSP questionnaire. In this study, each participant was requested to give a daily score of 1 to 6 for each symptom in accordance with the severity across her menstrual cycle, the number 0 represented no symptoms, and higher numbers paralleled worsening of the symptoms. Clinical diagnostic interviews were then organized for each participant, during these interviews, the demographic information of each participant was collected. All patients were individually diagnosed by an experienced associate professor gynaecologist.

Participants without any treatment for at least 2 months consecutively prior to this study were enrolled from the local university. Thirty-six PMS patients and 36 matched HCs were accepted by this study. According to the G*Power instructions and one previous research of PMS ($1-\beta=0.80$, $\alpha=0.05$) (28), the sample size in this study has sufficient analytical power. The detailed inclusion criteria for PMS patients was: (I) the symptoms were concerned with abnormality in daily functioning, and contribute to the changes of affective (i.e., irritability, anxiety, depression and emotional instability), cognitive (i.e. had difficulty concentrating, felt overwhelmed or that I could not cope and felt out of control), physical (i.e., fatigued, changed appetite, sleep problems) or behavioral realm; (II) symptoms were alleviated later on the onset of menses and vacant during most of the mid-follicular phase of the menstrual period; (III) the symptoms were not merely a worsening of another physical chronic or mental disorders; (IV) age between 18 and 45; (V) the regular menstrual cycle range: 24–35 days; (VI) right-handedness; (VII) in most menstrual cycles, PMS occurred in 2 weeks before menstruation; and (VIII) menstrual-related periodicity, occurrence during the late luteal phase of cycle (days −7 to −1) and absence during the mid-follicular phase (days +1 to +7) for two consecutive menstrual cycles, were documented by repeated observations by the PMS patients basing on DRSP

criterion, and a mean luteal phase score at least 30% greater than that during the follicular phase.

The detailed exclusion criteria for PMS patients and HCs was: (I) irregular menstrual cycle; (II) contraindications to MRI scanning; (III) alcohol abusing or smoking; (IV) taking any pain medications, benzodiazepines, hormonal medications, steroid compound (e.g., hormonal intrauterine devices and oral contraceptives) or other medications affecting PMS; (V) being currently pregnant or lactating; (VI) having a history of gynecological inflammation, menopausal syndrome, dysmenorrhea, thyroid disease, bilateral oophorectomy or hysterectomy, cancer or mastopathy; (VII) having history of psychiatric disease diagnosed in line with Diagnostic and Statistical Manual of Mental Disorders (DSM)-5th Edition (29), such as organic mental disorder, schizophrenia, schizoaffective disorder, delusional mental disorder, psychotic features coordinated or uncoordinated with mood or bipolar disorder. During the recruitment process, patients with premenstrual dysphoric disorder (PMDD) were excluded from the participants according to the DSM-5.

HCs underwent the similar basic evaluations of inclusion mentioned above: (I) being right-handed; (II) age between 18 and 45; (III) the regular menstrual cycle range: 24–35 days.

Imaging acquisition

The MRI data of all participants were conducted on a 3T Siemens Magnetom Verio MRI System (Siemens Medical, Erlangen, Germany) equipped with eight-channel phased-array head coil. Resting-state functional magnetic resonance imaging (fMRI) data were collected through a single-shot gradient-recalled echo planar imaging (EPI) sequence with the following parameters: flip angle (FA) =90°; field of view (FOV) =240 mm × 240 mm; repetition time (TR) =2,000 ms; echo time (TE) = 30 ms; matrix =64×64; slices =31, slice thickness =5 mm, no-gap, and total of 180 volumes. High resolution T1-weighted images were then acquired by employing a volumetric three-dimensional (3D) spoiled gradient recall sequence with the following parameters: FA =9°, FOV =250 mm × 250 mm, TR =1,900 ms; TE =2.22 ms, matrix size: 250×250, slices =176, slice thickness =1 mm, and no-gap. The total scanning time was about 6 minutes. During the scanning, the participants were instructed to remain motionless, not to consider anything, keep eyes closed and avoid falling to sleep. Foam pillows were applied to minimize movement between the instrument and each participant's head.

Functional data preprocessing

The resting-state fMRI data were pre-processed based on Statistical Parametric Mapping (SPM12, UK, http://www.fil.ion.ucl.ac.uk/spm) using the Data Processing Analysis of Brain Imaging (DPABI 4.3; http://rfmri.org/dpabi). Converted the raw DICOM data into the NIFTI data format. To allow for magnetization equilibrium and participant familiarization, the first 5 volumes for each participant were discarded. The remaining 175 volumes were corrected for slice timing and head motion correction. Discarded the head translation movement was >2.5 mm and rotation was >2.5° for all participants. Next, all data were spatially normalized to the Montreal Neurological Institute (MNI) space (EPI template with 3 mm × 3 mm × 3 mm voxel size). Furthermore, removal of linear trends of the blood oxygenation level-dependent signal of each voxel. Nuisance regressions (Friston-24 parameters, cerebrospinal fluid signals, white matter) and band-pass filtering were performed.

Structural data preprocessing

The sMRI date were performed using the Computational Anatomy Toolbox 12 (CAT12, http://dbm.neuro.uni-jena.de/cat) implemented with statistical parametric mapping (SPM12, http://www.fil.ion.ucl.ac.uk/spm/software/spm12). Each participant's MRI data were segmented into GM, white matter, and cerebrospinal fluid. High-dimensional Diffeomorphic Anatomical Registration Through Exponential Lie Algebra (DARTEL) algorithm by linear and non-linear transformation, the native-space structural MRI images were transformed into the MNI 152 standard space, and segmented to GM of 1.5 mm × 1.5 mm × 1.5 mm voxels. Furthermore, CAT12 was applied to display all slices for all images and to calculate the homogeneity of obtained GM maps between participants. After correcting for bias-field inhomogeneities, the normalized and modulated GM images were smoothed with a 6 mm isotropic Gaussian kernel.

Calculation of FCD maps

The voxel-based FCD maps of each participant were calculated for each voxel using the in-house script in line with previous researches (11,12). FCD maps including LFCD map and global FCD (GFCD) map for each participant were conducted within a GM mask on the basis

of preprocessed images (11,12). The LFCD at a given voxel x_0 was defined as the local number connections, $k(x_0)$, between x_0 and its adjacent voxels represented by the 3D searching algorithm. The GFCD calculations were confined to voxels within the GM mask, and the GFCD at any given voxel x_0 was computed using a growth algorithm to identify the total number of functional connections $k(x_0)$ based on Pearson's correlation (between x_0 and all other voxels with an absolute correlation coefficient value >0.6 were considered functionally connected); this procedure was repeated for all x_0 voxels. The LRFCD was defined as the GFCD minus LFCD. To reduce the effect of individual variability and increase the normality, the LFCD and LRFCD maps of each participant were standardized. Finally, to minimize the differences in the functional anatomy of the brain across participants, the standardized LFCD and LRFCD maps were spatially smoothed with a 6-mm isotropic Gaussian kernel.

Statistical analysis

Demographic characteristics and clinical data of the PMS patients and HCs were examined by SPSS software (version 22.0; IBM, Armonk, New York). Two-sample two-tailed *t*-test was applied to compare the significant differences of demographic characteristics and clinical variables between PMS and HCs. The statistical threshold was set at P<0.05 for all comparisons.

In SPM12, separate repeated-measures two-way analysis of variance (ANOVA) was conducted for both LFCD and LRFCD measures with group (two levels: PMS and HCs) as a between-subject factor, and frequency bands (two levels: slow-4 and slow-5) as a repeated-measures factor, with age, height and weight as insignificant covariates (11,30) [P<0.05, family-wise error (FWE) corrected; or with a voxel P<0.005, and a cluster level P<0.05, Gaussian random field (GRF) corrected]. The surviving brain clusters were selected as the regions of interest (ROIs) for the following post-hoc analysis, two-sample two-tailed t tests were performed on: (I) these main effect ROIs to determine the differences between the groups (PMS and HCs); (II) these interaction effect ROIs to ascertain the differences between the groups (PMS and HCs) and frequency bands (slow-4 and slow-5).

Furthermore, based on the post-hoc analysis of frequency-specific alteration FCD, the receiver operating characteristic (ROC) curves were generated to assess whether the FCD alteration of each observed ROI could be used to identify PMS patients from the controls [including 95% confidence interval (CI), P value and area under the ROC curve (AUC)]. Nonparametric permutation test was applied to examine the statistical significance (P<0.05).

The higher AUC value of the specific ROIs which indicates higher precision in terms of identifying PMS patients from the HCs (i.e., the striatum in this study). Based on the ROC results, we thereby investigated the structural covariance of striatum subregions between the PMS patients and HCs. First, four caudate subregions (dorsal caudate: ROI 1–2; ventral caudate: ROI 3–4), four putamen subregions (dorsolateral putamen: ROI 5–6; ventromedial putamen: ROI 7–8) and bilateral pallidum (ROI 9–10) were defined on the basis of the Human Brainnetome Atlas (*Figure 1*) (http://atlas.brainnetome.org/bnatlas.html). Second, two tailed two-sample *t*-tests were applied to compare the mean GM volumes (GMV) differences of ten striatum subregions (ROI 1–10) between PMS patients and HCs (Bonferroni corrected, P<0.05). Third, whole-brain structural covariance analyses were performed to investigate abnormal patterns of each subregions showing significant GMV-group differences. Multiple regression models were established on the modulated GM images for each group using the general linear model in SPM12. The mean GMV from each ROI was included in these regression models as a covariate of interest within each group, and age, height, weight and total intracranial volume (TIV) were seen as covariates of no interest in each regression model (31). One-sample *t*-test was used to produce structural covariance maps. Only significantly positive covariance patterns with the mean GMV of each ROI was reserved in each group (P<0.05, false discovery rate (FDR) corrected; or with a voxel P<0.005, and a cluster level P<0.05, GRF corrected).

Furthermore, the between-group differences in structural covariance were evaluated by the different slopes for any pair of regions in accordance with previous studies (32,33). Thereby, in order to evaluate the difference of structural covariance between-groups, we performed a between-group analysis of slopes by using a multiple classic linear interaction model:

$$Y = \beta_0 + \beta_1 X + \beta_2 G + \beta_3 (GX) + \beta_4 Age + \beta_5 Height + \beta_6 Weight + \beta_7 TIV + \varepsilon \quad [1]$$

In this model, Y indicated a vector of the GMV of each region showing between-group differences; X represented the averaged GMV in each seed; G was a vector with binary group labels, and two groups were put into the same model (where 1 indicating PMS patients and –1 indicating HCs). In consistent with previous studies, age, height, weight and

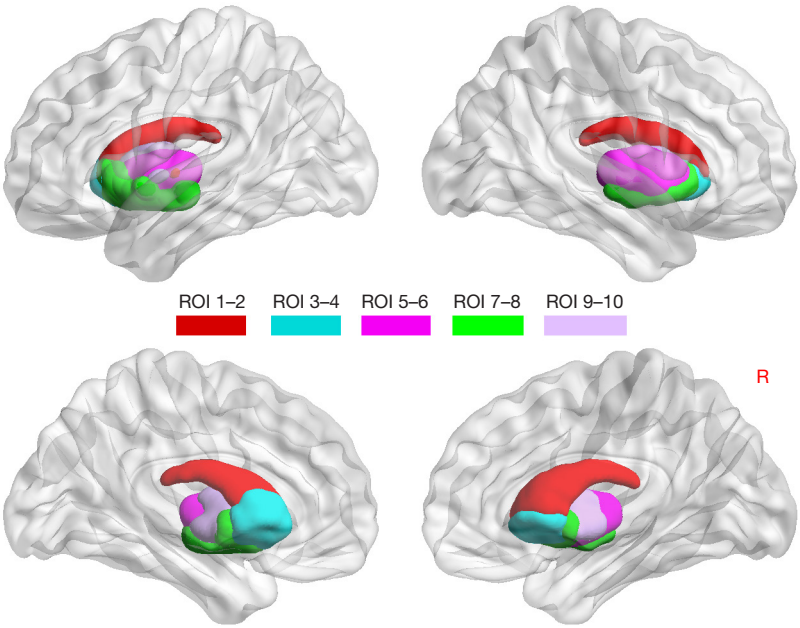

Figure 1 The anatomical location of striatum subregions. The striatum subregions containing the four caudate subregions (dorsal caudate: ROI 1–2; ventral caudate: ROI 3–4), four putamen subregions (dorsolateral putamen: ROI 5–6; ventromedial putamen: ROI 7–8) and bilateral pallidum (ROI 9–10). ROI, region of interest; R, right.

TIV were included as nuisance variables (31). β_3 modeled the relationship between the interaction term Group-by-X (32,33). Specific *t*-value of β3 as the statistic to perform a permutation test (1,000 times; P<0.05).

Pearson's correlation analyses were performed between the mean LFCD/LRFCD value and striatum subregions GMV that showed significant difference and the DRSP (i.e., DRSP total score, sub-symptom scores of DRSP and subscale scores of physical symptoms) scores of PMS patients (Bonferroni corrected, P<0.05).

Results

Demographic characteristics and clinical variables

The number of participants at each stage were reported by a flow diagram of *Figure 2*. Finally, 35 PMS patients and 36 HCs were enrolled in this study. Demographic characteristics and clinical variables of PMS patients and HCs are summarized in *Table 1*. There was no significant difference in terms of age, height, weight, menophania and menstruation (P>0.05) (*Table 1*). The PMS patients had a higher length of menstrual cycle than HCs (P=0.04) (*Table 1*). The self-rating anxiety scale (SAS) score, self-rating depression scale (SDS) score and total DRSP scores in the late luteal phase of PMS patients were significantly higher than HCs (P<0.001) (*Table 1*). The sub-symptom (affective symptoms, physical symptoms, cognitive changes and behavioral realm) scores of DRSP and subscale scores of physical (i.e., fatigued, changed appetite and sleep problems) in the late luteal phase of PMS patients were significantly higher than HCs (P<0.001) (*Table 1*).

Main effects of group

A significant LFCD main effect of group is shown in *Figure 3A* and Table S1. PMS patients exhibited significantly decreased LFCD in the left middle cingulate cortex (MCC) compared with HCs (*Figure 3B*). A significant LRFCD main effect of group is shown in *Figure 3C* and Table S1. PMS patients exhibited significantly increased LRFCD in the left PreCG compared with HCs (*Figure 3D*).

Interaction effects between the frequency band and group

Significant LFCD frequency-by-group interaction effect is observed in *Figure 4A* and Table S2. PMS patients showed significantly decreased LFCD in the striatum (including the left caudate, left putamen, left pallidum) and left

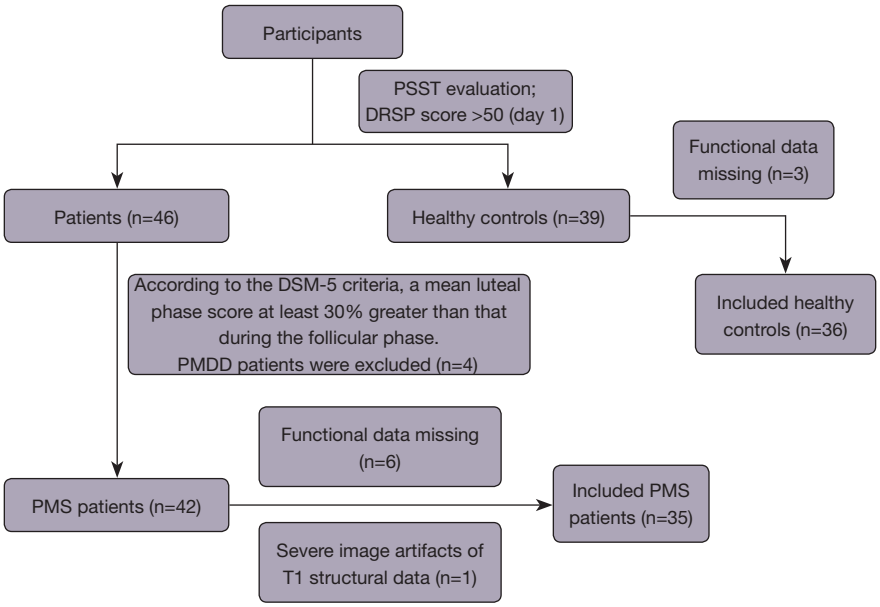

Figure 2 The flow diagram to report the number of participants at each stage in this study. PSST, Premenstrual Syndrome Scales Tool; DRSP, daily record of severity of problems; DSM-5, Diagnostic and Statistical Manual of Mental Disorders-5th Edition; PMDD, premenstrual dysphoric disorder; PMS, premenstrual syndrome.

Table 1 Demographic and clinical characteristics for PMS patients and HCs

Characteristics	PMS (n=35)	HCs (n=36)	P value
Age (years)	24.29±2.75	23.64±1.74	0.24
Height (cm)	158.31±5.47	157.78±4.34	0.65
Weight (kg)	51.40±7.83	51.83±8.31	0.82
Menophania (years)	12.89±1.05	12.89±1.01	0.99
Menstruation (days)	6.20±1.21	5.94±1.15	0.36
Length of menstrual cycle (days)	30.77±2.29	29.72±1.97	0.04
SAS	48.77±8.47	36.72±8.01	<0.001***
SDS	55.20±10.03	42.11±10.15	<0.001***
Total DRSP score	67.42±13.42	28.60±5.21	<0.001***
Sub-symptom scores of DRSP			
Affective symptoms	162.40±38.47	56.56±7.64	<0.001***
Physical symptoms	171.83±35.86	78.53±18.20	<0.001***
Cognitive changes	57.26±19.24	23.97±4.27	<0.001***
Behavioral Realm	92.26±21.74	36.39±4.70	<0.001***
Subscale scores of physical			
Fatigued etc.	22.51±5.63	9.07±3.20	<0.001***
Changed appetite	36.90±14.51	18.40±6.42	<0.001***
Sleep problems	42.57±10.90	18.19±5.19	<0.001***

Date are shown as mean ± SD. ***, P<0.001 obtained by two-sample two-tailed *t*-test. PMS, premenstrual syndrome; HCs, healthy controls; SD, standard deviation; SAS, self-rating anxiety scale; SDS, self-rating depression scale; DRSP, daily record of severity of problems.

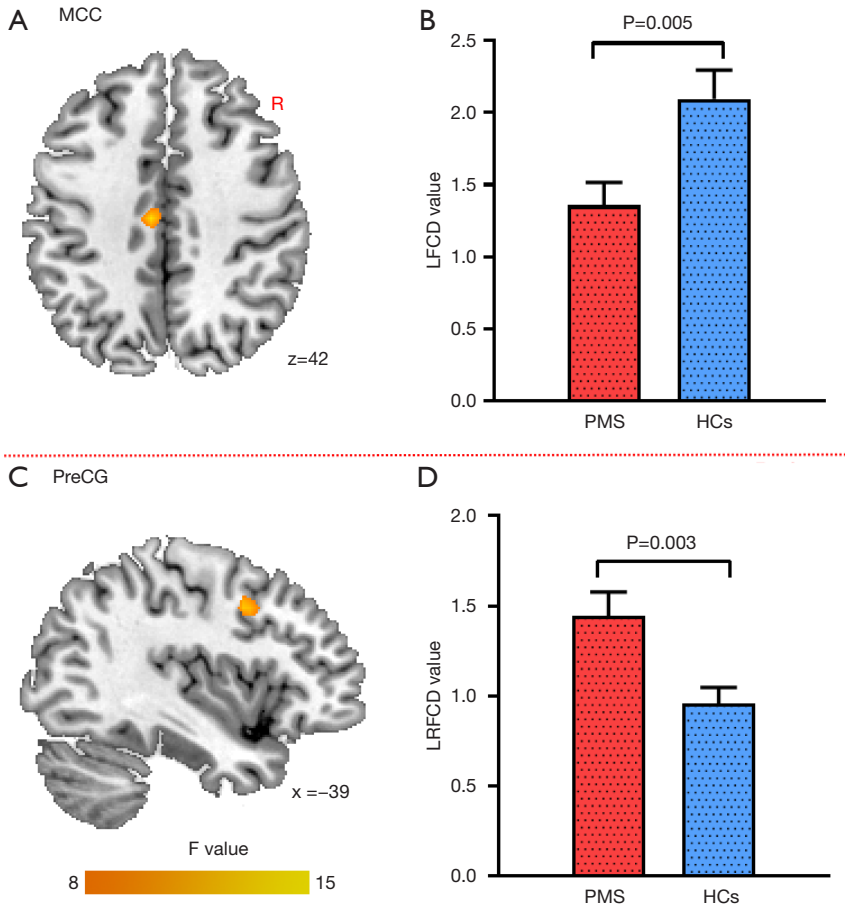

Figure 3 Main effect of the group on LFCD and LRFCD. The results were obtained by repeated-measures two-way ANOVA. Main effect of group on LFCD (A) and LRFCD (C); as well as *post-hoc* analysis of the group on LFCD (B) and LRFCD (D). ANOVA, analysis of variance; PMS, premenstrual syndrome; HCs, healthy controls; MCC, middle cingulate cortex; PreCG, precentral gyrus; R, right; LFCD, local functional connectivity density; LRFCD, long-range functional connectivity density.

thalamus in the slow-5 frequency band in comparison with HCs; and no significant different LFCD of these regions was found in the slow-4 frequency band (*Figure 4B*). The significant LRFCD frequency-by-group interaction effect is observed in *Figure 4C* and Table S2. PMS patients showed significantly increased LRFCD in the right OFC in the slow-4 band whereas no significantly altered LRFCD in this cluster in the slow-5 in comparison with HCs (*Figure 4B*).

ROC analysis results

In slow-5 band, the ROC results showed that the LFCD of striatum and thalamus regions could potentially be recognized as markers to distinguish PMS patients from HCs in *Figure 5*. The AUC values (95% CI, P value) of these regions from ROC analysis were 0.744 (0.630–0.857, P<0.001) in the left caudate, 0.756 (0.644–0.869, P<0.001) in the left putamen, 0.733 (0.617–0.850, P=0.001) in the left pallidum, and 0.726 (0.609–0.843, P=0.001) in the left thalamus.

GMV differences and structural association of striatum between groups

PMS patients showed decreased GMV in the four caudate subregions (ROI 1–4) than HCs (Bonferroni corrected, P<0.05, *Figure 6*). The detailed structural covariance patterns of the four caudate subregions in PMS and HCs were mainly located in the caudate, pallidum, thalamus and frontal lobe (Figure S1 and Figure S2).

Compared with HCs, the results of interaction linear

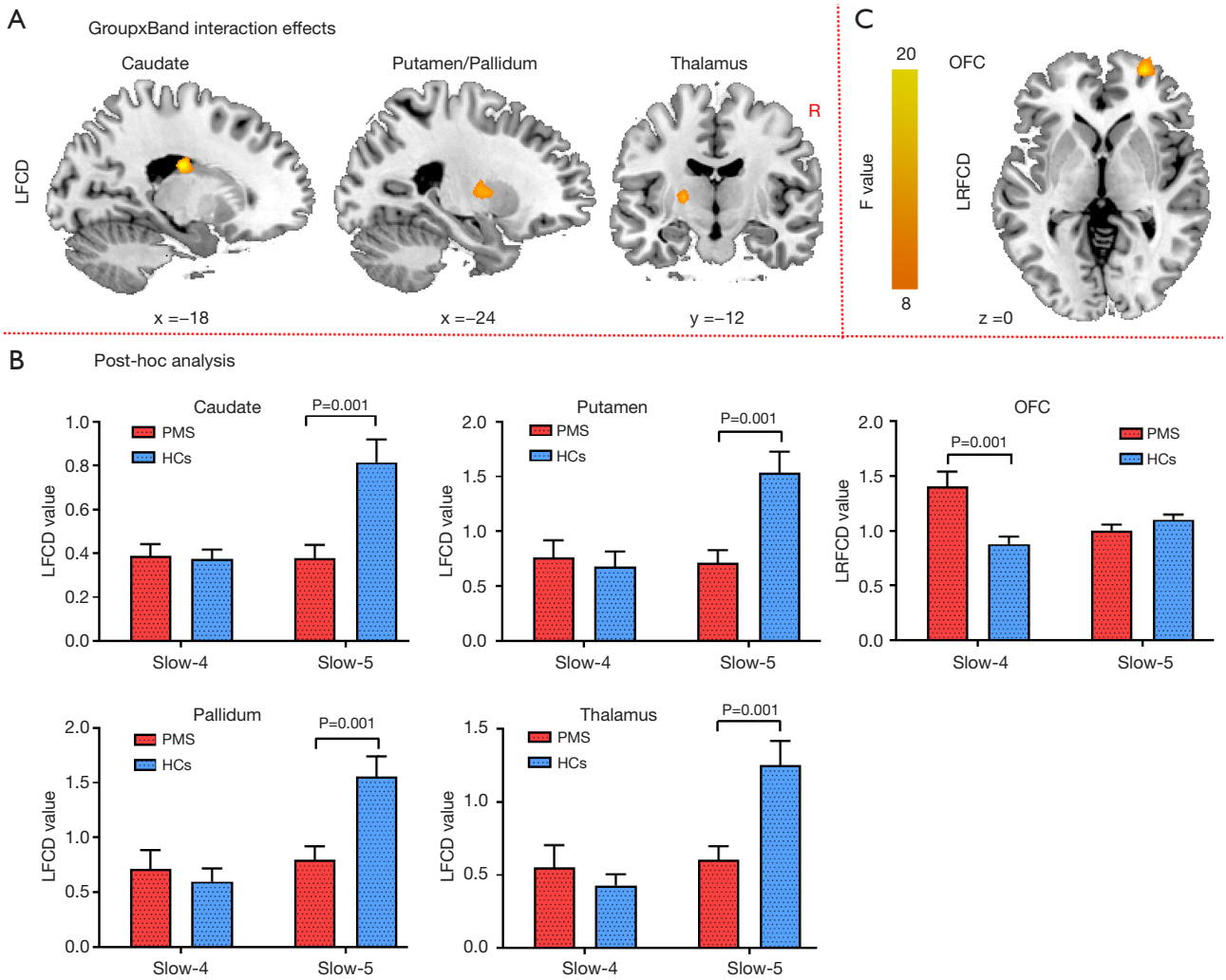

Figure 4 Interaction effect between the frequency band (slow-4 and slow-5) and the group (PMS and HCs) on LFCD and LRFCD. The results were obtained by repeated-measures two-way ANOVA. The interaction between the frequency band and diagnosis on LFCD (A) and LRFCD (C); as well as the *post-hoc* analysis of the interaction effect (B). ANOVA, analysis of variance; PMS, premenstrual syndrome; HCs, healthy controls; OFC, orbitofrontal cortex; R, right; LFCD, local functional connectivity density; LRFCD, long-range functional connectivity density.

model analysis showed that PMS patients had the decreased covariance between the bilateral dorsal caudate, left ventral caudate and the right MFC, and the decreased covariance between the left ventral caudate and the left MPFC (*Figure 7*).

Correlation between imaging results and clinical symptoms

The LFCD value in the left thalamus in the slow-5 band in PMS patients was significantly negatively correlated with the scores of physical symptoms (r=−0.39, P=0.021) (*Figure 8*) and the scores of sleep problems (subscale of physical symptoms) (r=−0.43, P=0.009) (*Figure 8*).

Discussion

This study applied voxel-based FCD and structural covariance analysis to investigate possibly altered FC and structural covariance patterns among PMS patients and HCs.

Group differences in FCD between PMS and HCs

FCD provides an unbiased fMRI feature to characterize the

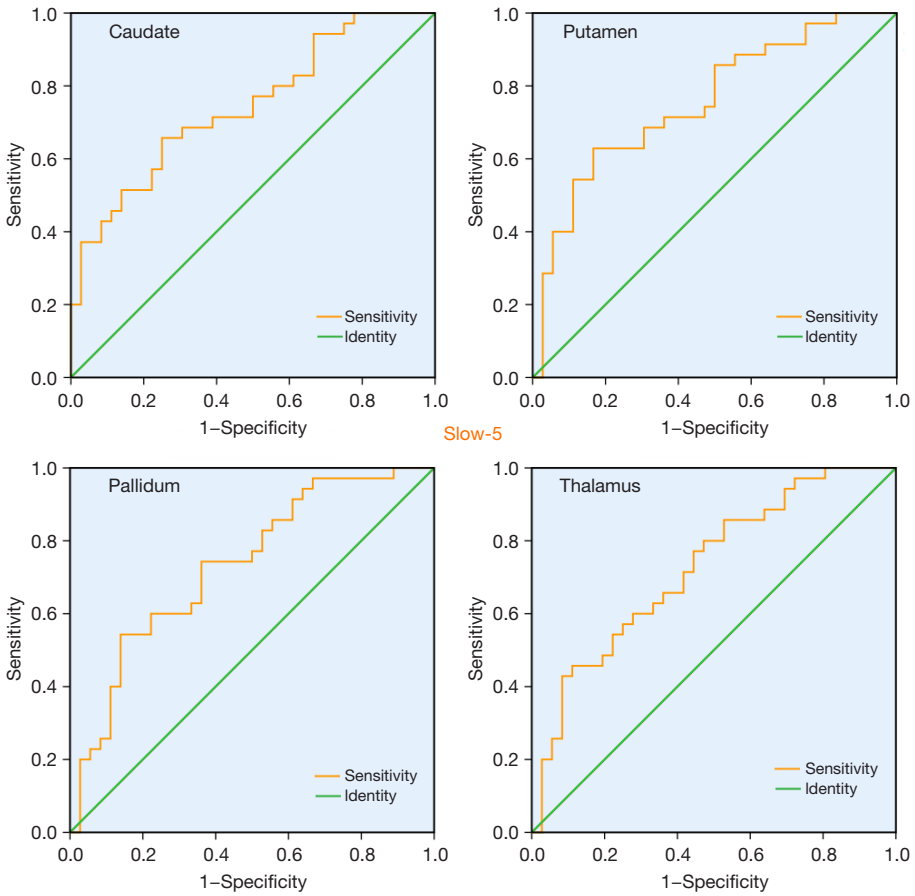

Figure 5 In the slow-5 frequency band, ROC curve analysis results of differentiating the PMS patients from the HCs by using the LFCD based on the four regions (left caudate, left putamen, left pallidum and left thalamus). The orange lines represent the sensitivity of each specific brain region in ROC analysis, and the green lines represent the identity of each specific brain region in ROC analysis. ROC, receiver operating characteristic; PMS, premenstrual syndrome; HCs, healthy controls; LFCD, local functional connectivity density.

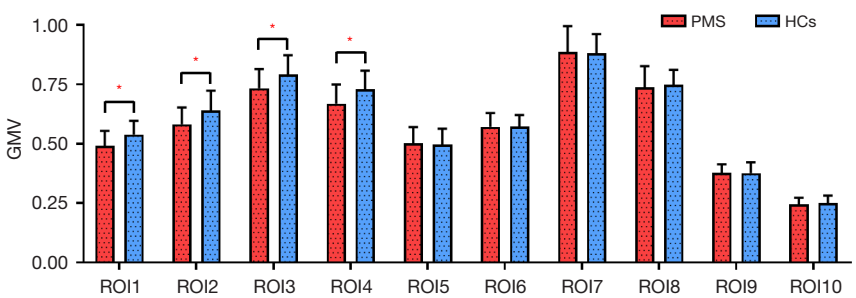

Figure 6 The GMV differences between groups in the striatum subregions. The GMV differences between PMS patients and HCs in the striatum subregions. *, P<0.005 (Bonferroni corrected, P<0.05). GMV, gray matter volume; ROI, region of interest; PMS, premenstrual syndrome; HCs, healthy controls.

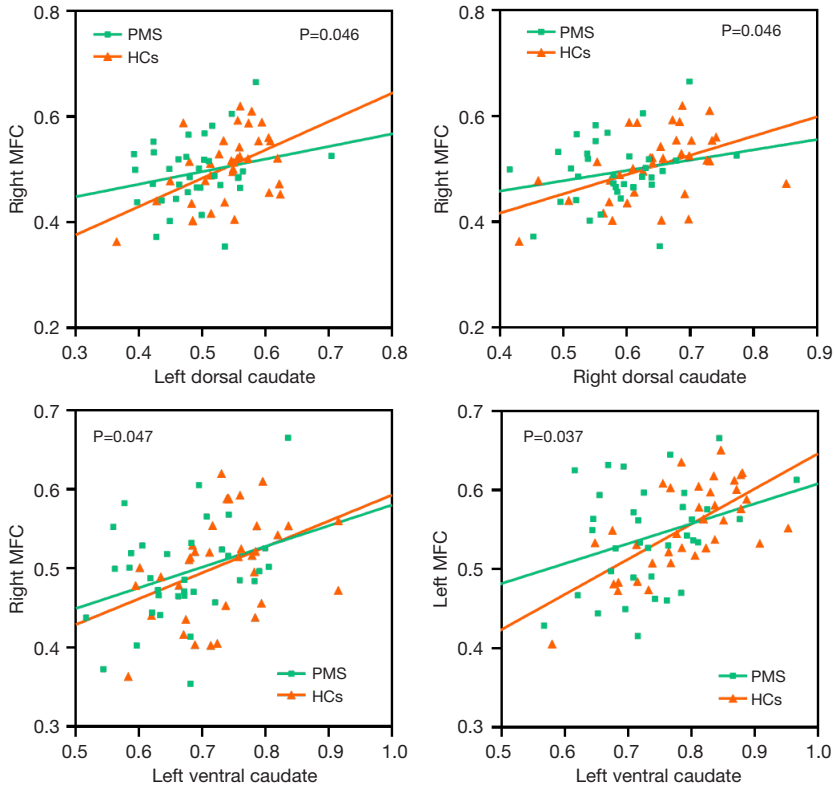

Figure 7 Significant between-group differences in structural covariance for PMS and HCs. Specific regions showed significant between-group differences with the caudate subregions. PMS, premenstrual syndrome; HCs, healthy controls; MFC, middle frontal cortex.

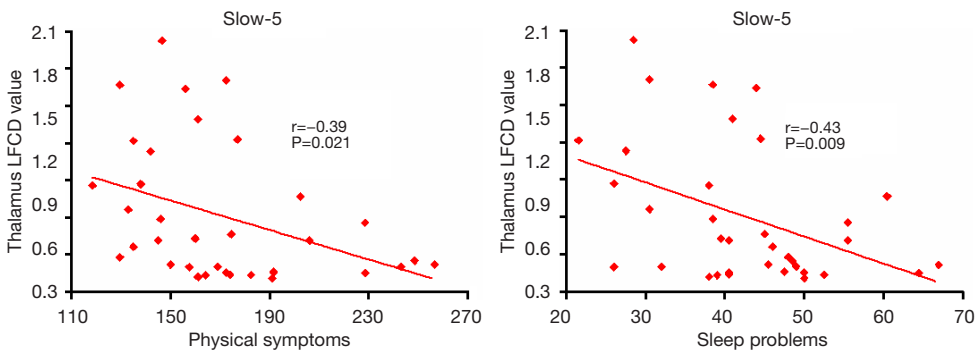

Figure 8 In the slow-5 frequency band, negative correlation between the LFCD of the thalamus and sub-symptom scores of DRSP (i.e., the physical symptoms, especially for the sleep problems) in patients with PMS (Bonferroni corrected, P<0.05). PMS, premenstrual syndrome; LFCD, local functional connectivity density; DRSP, daily record of severity of problems.

voxel-based FC in brain (11). In the present study, we found decreased LFCD in the MCC in PMS patients. As a pivotal component of homeostatic afferent network and emotional-arousal network, the MCC is associated with appraising the importance of visceral stimulation and emotional regulation (34). Duan *et al.* reveled the aberrant hippocampus-MCC connectivity was implicated in the impaired somatic sensation processing in PMS patients (6).

Increased LRFCD in the PreCG was also found in PMS patients in this study. Recent studies have shown that LRFCD captures long distance brain communication which requires higher time and metabolic costs than LFCD (35,36). The disruption in the balance between LRFCD and LFCD may imply a shift between the costly metabolic connection and economic connection (30). The PreCG is one key region of somatosensory cortex, which responds to sensory and motor processing. The MCC was also positively correlated with the sensorimotor networks (37). The somatosensory cortex, displaying high local connectivity, was implicated in the neuropsychiatric disorders (38). Numerous studies have proved that the PreCG not only encodes bodily sensations, but also plays an important role in understanding and recognizing other's emotional states utilizing social cues (39-41), and dysfunction of PreCG may be associated with hypoesthesia or sensory disorder depression patients. Previous studies have indicated that PMS patients exhibit a blunted response in the sympathetic system when they experience acute stressors (42,43). Dubol *et al.* reviewed the neuroimaging evidence for PMDD (the most severe form of PMS) and found that the PreCG was concerned with the severity of PMDD, implying a reduced cognitive control over the negative stimulation in women with premenstrual disorders (44). Meng *et al.* reported that the significant lower activation in the PreCG in PMS patients than HCs during stress condition, and indicated the insensitive response of the nervous system might be considered as one of the reasons for a decreased cognitive control of premenstrual disorders (28). Cognitive change is also integrated with negative emotion processing and psychiatric symptoms such as anxiety and depression (45). Thereby, the disruption in the balance between LFCD in the MCC and LRFCD in the PreCG may be involved in the somatosensory processing and negative emotion, that might contribute to the dysregulation of visceral sensory afferent responses of PMS patients. However, more evidence is needed to further verify "the imbalance between the LFCD and LRFCD in PMS" in the future. Predicting that long-range connectivity but shorter local connectivity is worse for emotional regulation may be a valuable topic in the future studies.

Frequency-specific changes in FCD in PMS

Another remarkable finding in the present study was that the changed LFCD in the striatum and thalamus were modulated by the frequency bands. The striatum, thalamus and OFC play crucial characters in the cortico-striatal-thalamic-cortical (CSTC) network. The CSTC network, which was implicated in emotional, cognitive and sensorimotor functions (46,47), plays a key role in the pathophysiology of affective disorders, such as major depressive disorder (48), Parkinson's disease related-anxiety (23). Recently, one research reported a significant interaction between the frequency band and group in the caudate in Parkinson's disease with depression patients, and suggested that the slow-5 band was more suitable for detecting degree centrality abnormalities associated with the CSTC network (49). Zhang *et al.* indicated a significant interaction between the frequency band and group in the striatum and thalamus in patients with social anxiety disorder generated by different mechanisms (50). These findings indicated that the pattern of intrinsic brain connectivity was sensitive to the specific frequency band. Moreover, in our study, the ROC results demonstrated that the striatum had the well performance to distinguish the patients from HCs, indicating the LFCD in the striatum could be potential biomarkers for PMS in slow-5 band. Accordingly, this study argues that the slow-5 band might have greater sensitivity in detecting the alterations of functional communication of CSTC network in PMS patients than the slow-4 band.

In addition, this study discovered the significant interaction of the LRFCD in the OFC between the slow-4 and slow-5 bands in PMS patients compared with HCs. The OFC, having specific connections within the CSTC network, contributes to regulate the interactions between emotional processing and cognitive functions (51,52). The disruption of long-range information interaction is associated with the reduction of brain network efficiency and may bring on aberrant cognition and clinical characteristics in mental diseases (16,35). One recent research reported that the increased LRFCD in OFC might be prejudicial to the diversity of inputs and outputs in brain areas in human (53). Another study from Gingnell *et al.* revealed hyperactivations of the OFC in PMDD patients during the anticipation of negative pictures during the luteal phase (54). Moreover, one previous study showed that the similar pattern of "hyperconnectivity" in the OFC provided a possible explanation for the social cognition abnormalities (15). Therefore, the dissimilarities of PMS-related long-range information interaction between frequency bands suggests that the alterations in brain connectivity in PMS patients may be strongly modulated by the frequency bands. The properly chosen frequency band would be helpful to explore

PMS-related neural mechanism more sensitively. The current results might present the disturbed modulation function of the OFC in PMS and may be correlated with the dysregulation of cognitive in such disease.

Changed structural association of striatum subregions in PMS

PMS patients showed the decreased GMV in the caudate subregions compared with HCs. Furthermore, the decreased structural associations between the caudate subregions and frontal lobe (MFC and MPFC) were found in PMS compared with HCs. Previous studies proved that the dorsal and ventral caudate demonstrate different vulnerability to diseases, specifically, the dorsal caudate appears to be more vulnerable to diseases that cause cognitive impairments (e.g., Parkinson's disease) (55), while the ventral caudate appears more disrupted in affective disorders (such as obsessive-compulsive disorder and major depression) (56). It was proved that the MFC had specific influence on cognitive and emotional functions in the menstrual cycle (57). The MPFC is implicated in cognitive and emotional processing, and MPFC-related hypoactivation may contribute to anhedonia symptoms (58). Liu *et al.* found the reduced cortical thickness in the MPFC, which was associated with impaired menstrual cycle-related emotion regulation in PMS (9). Furthermore, the ventral caudate is involved in the affective functions including the perception of fatigue (59). Particularly, clinical assessment of fatigue is significantly correlated with neural activity in the ventral caudate during hedonic reward tasks (60). In the present study, the significant higher fatigue and less interest in usual activities (e.g., work, school, friends and hobbies) were found in PMS patients compared with HCs. There is accumulating evidence suggesting that hormones fluctuations (particularly estradiol and progesterone) across women menstrual cycle leading to frontal lobe GM reductions (61-64). Taken together, we speculate that the decreased GMV of caudate subregions and decreased structural association between caudate-frontal lobe in PMS may be associated with the menstrual cycle-related dysregulation of emotion, and thus contribute to the less interest in usual activities and higher perception of fatigue.

Correlation between imaging results and clinical symptoms

Interestingly, in the slow-5 band, the decreased LFCD in the thalamus was negatively correlated with the severity of sleep problems in patients with PMS. As a vital region in integrating neural activity from widespread neocortical inputs and outputs, the thalamus is considered to play a main character in adjusting state of sleep and wakefulness. Recently, in the classical frequency band, Kong *et al.* revealed that the altered short-range FCD in thalamus was associated with cognitive function in healthy subjects after acute sleep deprivations (65). In particular, the thalamus is the integral component within the limbic CSTC network, and it transmits sensory salience information to the prefrontal cortex. To protect sleep from external interference, the thalamus selects information to be projected to the cortex while the cortex is asleep (66). Negative correlation demonstrates that as the severity of sleep problems increases, the function communication in the thalamus area becomes less. The significantly higher scores of physical symptoms (such as fatigued, had trouble getting to sleep or staying asleep) of PMS than HCs were found in the present study. Taken together, these findings might suggest that the disturbed function communication in thalamus is dependent on the frequency bands, which enhances our understanding of frequency-specific pathology of PMS. The underlying neural mechanisms of this interaction in thalamus and frequency domains of PMS are interesting topics that require further investigations.

Several limitations of the current work should be acknowledged. Firstly, we recruited participants of this study during their late luteal phase. However, the evaluation of hormone levels of participants was not performed in our experimental design. Women had obvious hormonal fluctuations during the menstrual cycle, which is known that hormonal fluctuations may affect neural plasticity on women's brain (61-64). The study merely investigated the brain functional and structural changes of PMS patients at luteal phase by comparing to HCs. It remains to be further studied and confirmed whether the results are partially due to the hormones fluctuations across menstrual cycle in future works. Secondly, we could not eliminate completely the effects of the physiological noise, such as cardiac and respiratory pulsation, from the resting-state fMRI data of slow-4 and slow-5 frequency bands. Thirdly, although age, height and weight were regressed as covariates in ANOVA analysis, it is difficult to exclude such inherent differences among individuals. Fourthly, the sample size in this study is relatively small. Further study with larger clinical dataset may provide more sufficient power and external validity for image analysis and draw more definitive conclusions. Fifthly,

in the present study, the recruited women with a relatively narrow age range, which may limit the generalizability of the neuroimaging findings. Thus, a more extensive age range of participants will be enrolled in future work. Finally, there were relatively low amounts of fMRI data collected for each individual (180 images, 6 min scan time, TR =2 seconds) in this study. Therefore, further study with higher amounts of fMRI data to verify the reliability and validity of this study results.

Conclusions

In summary, based on multi-modal MRI, we explored the frequency-specific FCD and structural covariance patterns in PMS patients. The abnormal functional communication was found in the MCC and PreCG. The significant frequency band-by-group interaction effect was mainly located in the striatum, thalamus and OFC. Moreover, the result from the ROC analysis might explore the core roles of striatum in the pathophysiology of PMS in slow-5 band. The decreased structural covariance was found between the striatum (i.e., caudate) subregions and frontal lobe. Interestingly, the LFCD in the thalamus was significantly negatively correlated with the sleep problems in slow-5 band. This neuroimaging study imply the abnormal emotional regulation and aberrant cognitive function related to PMS. Our neuroimaging findings suggest that frequency-specific FCD and structural covariance analysis might improve our understanding of the pathophysiologic mechanism of PMS from novel perspective.

Acknowledgments

The authors would like to express their gratitude for the support of these projects.
Funding: This study was financially supported by the National Natural Science Foundation of China (Nos. 82270696, 82060315, 81760886, 82102032 and 81960570); Guangxi key research and development program (No. AB22080053); Fundamental Research Funds for the Central Universities (No. XJS201202); and Natural Science Basic Research Program of Shaanxi (No. 2022JQ-649).

Footnote

Reporting Checklist: The authors have completed the STROBE reporting checklist. Available at https://qims.amegroups.com/article/view/10.21037/qims-22-506/rc

Conflicts of Interest: All authors have completed the ICMJE uniform disclosure form (available at https://qims.amegroups.com/article/view/10.21037/qims-22-506/coif). The authors have no conflicts of interest to declare.

Ethical Statement: The authors are accountable for all aspects of the work in ensuring that questions related to the accuracy or integrity of any part of the work are appropriately investigated and resolved. The study was conducted in accordance with the Declaration of Helsinki (as revised by 2013). This study was approved by the Medicine Ethics Committee of First Affiliated Hospital, Guangxi University of Chinese Medicine (No. 2018-037-02). Each participant was instructed to the whole experiment procedures and signed informed consent forms before experimentation.

References

1. Ryu A, Kim TH. Premenstrual syndrome: A mini review. Maturitas 2015;82:436-40.
2. Wu M, Liang Y, Wang Q, Zhao Y, Zhou R. Emotion Dysregulation of Women with Premenstrual Syndrome. Sci Rep 2016;6:38501.
3. Freeman EW. Premenstrual syndrome and premenstrual dysphoric disorder: definitions and diagnosis. Psychoneuroendocrinology 2003;28 Suppl 3:25-37.
4. Tolossa FW, Bekele ML. Prevalence, impacts and medical managements of premenstrual syndrome among female students: cross-sectional study in College of Health Sciences, Mekelle University, Mekelle, northern Ethiopia. BMC Womens Health 2014;14:52.
5. Rapkin AJ, Winer SA. Premenstrual syndrome and premenstrual dysphoric disorder: quality of life and burden of illness. Expert Rev Pharmacoecon Outcomes Res 2009;9:157-70.
6. Duan G, Liu H, Pang Y, Liu P, Liu Y, Wang G, Liao H, Tang L, Chen W, Mo X, Wen D, Lin H, Deng D.

Hippocampal fractional amplitude of low-frequency fluctuation and functional connectivity changes in premenstrual syndrome. J Magn Reson Imaging 2018;47:545-53.
7. Liu Q, Li R, Zhou R, Li J, Gu Q. Abnormal Resting-State Connectivity at Functional MRI in Women with Premenstrual Syndrome. PLoS One 2015;10:e0136029.
8. Liu C, Xuan C, Wu J, Li S, Yang G, Piao R, Duan G, Deng D, Liu P. Altered resting-state functional networks in patients with premenstrual syndrome: a graph-theoretical based study. Brain Imaging Behav 2022;16:435-44.
9. Liu P, Wei Y, Fan Y, Liao H, Wang G, Li R, Duan G, Deng D, Qin W. Cortical and subcortical changes in patients with premenstrual syndrome. J Affect Disord 2018;235:191-7.
10. Liu P, Wei Y, Fan Y, Li R, Liu Y, Wang G, Wei Y, Pang Y, Deng D, Qin W. Altered brain structure in women with premenstrual syndrome. J Affect Disord 2018;229:239-46.
11. Tomasi D, Volkow ND. Functional connectivity density mapping. Proc Natl Acad Sci U S A 2010;107:9885-90.
12. Tomasi D, Volkow ND. Association between functional connectivity hubs and brain networks. Cereb Cortex 2011;21:2003-13.
13. Guo S, Palaniyappan L, Yang B, Liu Z, Xue Z, Feng J. Anatomical distance affects functional connectivity in patients with schizophrenia and their siblings. Schizophr Bull 2014;40:449-59.
14. Chen SY, Cai GQ, Liang RB, Yang QC, Min YL, Ge QM, Li B, Shi WQ, Li QY, Zeng XJ, Shao Y. Regional brain changes in patients with diabetic optic neuropathy: a resting-state functional magnetic resonance imaging study. Quant Imaging Med Surg 2021;11:2125-37.
15. Wang X, Zhang Y, Long Z, Zheng J, Zhang Y, Han S, Wang Y, Duan X, Yang M, Zhao J, Chen H. Frequency-specific alteration of functional connectivity density in antipsychotic-naive adolescents with early-onset schizophrenia. J Psychiatr Res 2017;95:68-75.
16. Yang Y, Cui Q, Pang Y, Chen Y, Tang Q, Guo X, Han S, Ameen Fateh A, Lu F, He Z, Huang J, Xie A, Li D, Lei T, Wang Y, Chen H. Frequency-specific alteration of functional connectivity density in bipolar disorder depression. Prog Neuropsychopharmacol Biol Psychiatry 2021;104:110026.
17. Buzsáki G, Draguhn A. Neuronal oscillations in cortical networks. Science 2004;304:1926-9.
18. Zuo XN, Di Martino A, Kelly C, Shehzad ZE, Gee DG, Klein DF, Castellanos FX, Biswal BB, Milham MP. The oscillating brain: complex and reliable. Neuroimage 2010;49:1432-45.
19. Salvador R, Martínez A, Pomarol-Clotet E, Gomar J, Vila F, Sarró S, Capdevila A, Bullmore E. A simple view of the brain through a frequency-specific functional connectivity measure. Neuroimage 2008;39:279-89.
20. Han Y, Wang J, Zhao Z, Min B, Lu J, Li K, He Y, Jia J. Frequency-dependent changes in the amplitude of low-frequency fluctuations in amnestic mild cognitive impairment: a resting-state fMRI study. Neuroimage 2011;55:287-95.
21. Liu X, Wang S, Zhang X, Wang Z, Tian X, He Y. Abnormal amplitude of low-frequency fluctuations of intrinsic brain activity in Alzheimer's disease. J Alzheimers Dis 2014;40:387-97.
22. Mechelli A, Friston KJ, Frackowiak RS, Price CJ. Structural covariance in the human cortex. J Neurosci 2005;25:8303-10.
23. Oosterwijk CS, Vriend C, Berendse HW, van der Werf YD, van den Heuvel OA. Anxiety in Parkinson's disease is associated with reduced structural covariance of the striatum. J Affect Disord 2018;240:113-20.
24. Li R, Zou T, Wang X, Wang H, Hu X, Xie F, Meng L, Chen H. Basal ganglia atrophy-associated causal structural network degeneration in Parkinson's disease. Hum Brain Mapp 2022;43:1145-56.
25. World Medical Association Declaration of Helsinki: ethical principles for medical research involving human subjects. JAMA 2013;310:2191-4.
26. Bao AM, Ji YF, Van Someren EJ, Hofman MA, Liu RY, Zhou JN. Diurnal rhythms of free estradiol and cortisol during the normal menstrual cycle in women with major depression. Horm Behav 2004;45:93-102.
27. Endicott J, Nee J, Harrison W. Daily Record of Severity of Problems (DRSP): reliability and validity. Arch Womens Ment Health 2006;9:41-9.
28. Meng Y, Huang D, Hou L, Zhou R. Hypoactivation of autonomtic nervous system-related orbitofrontal and motor cortex during acute stress in women with premenstrual syndrome. Neurobiol Stress 2021;15:100357.
29. Association AP. Diagnostic and Statistical Manual of Mental Disorders, 5th edition. Washington, DC: American Psychiatric Press, 2013.
30. Liu D, Chen L, Duan S, Yin X, Yang W, Shi Y, Zhang J, Wang J. Disrupted Balance of Long- and Short-Range Functional Connectivity Density in Type 2 Diabetes Mellitus: A Resting-State fMRI Study. Front Neurosci 2018;12:875.

31. Montembeault M, Joubert S, Doyon J, Carrier J, Gagnon JF, Monchi O, Lungu O, Belleville S, Brambati SM. The impact of aging on gray matter structural covariance networks. Neuroimage 2012;63:754-9.
32. Wang X, Yu Y, Zhao W, Li Q, Li X, Li S, Yin C, Han Y. Altered Whole-Brain Structural Covariance of the Hippocampal Subfields in Subcortical Vascular Mild Cognitive Impairment and Amnestic Mild Cognitive Impairment Patients. Front Neurol 2018;9:342.
33. Ge R, Hassel S, Arnott SR, Davis AD, Harris JK, Zamyadi M, Milev R, Frey BN, Strother SC, Müller DJ, Rotzinger S, MacQueen GM, Kennedy SH, Lam RW, Vila-Rodriguez F. Structural covariance pattern abnormalities of insula in major depressive disorder: A CAN-BIND study report. Prog Neuropsychopharmacol Biol Psychiatry 2021;111:110194.
34. Elsenbruch S, Rosenberger C, Enck P, Forsting M, Schedlowski M, Gizewski ER. Affective disturbances modulate the neural processing of visceral pain stimuli in irritable bowel syndrome: an fMRI study. Gut 2010;59:489-95.
35. Wang S, Zhan Y, Zhang Y, Lyu L, Lyu H, Wang G, Wu R, Zhao J, Guo W. Abnormal long- and short-range functional connectivity in adolescent-onset schizophrenia patients: A resting-state fMRI study. Prog Neuropsychopharmacol Biol Psychiatry 2018;81:445-51.
36. Tomasi D, Volkow ND. Reduced Local and Increased Long-Range Functional Connectivity of the Thalamus in Autism Spectrum Disorder. Cereb Cortex 2019;29:573-85.
37. Yu C, Zhou Y, Liu Y, Jiang T, Dong H, Zhang Y, Walter M. Functional segregation of the human cingulate cortex is confirmed by functional connectivity based neuroanatomical parcellation. Neuroimage 2011;54:2571-81.
38. Sepulcre J, Liu H, Talukdar T, Martincorena I, Yeo BT, Buckner RL. The organization of local and distant functional connectivity in the human brain. PLoS Comput Biol 2010;6:e1000808.
39. Keysers C, Kaas JH, Gazzola V. Somatosensation in social perception. Nat Rev Neurosci 2010;11:417-28.
40. Jiang W, Yin Z, Pang Y, Wu F, Kong L, Xu K. Brain functional changes in facial expression recognition in patients with major depressive disorder before and after antidepressant treatment: A functional magnetic resonance imaging study. Neural Regen Res 2012;7:1151-7.
41. Fujino J, Yamasaki N, Miyata J, Kawada R, Sasaki H, Matsukawa N, Takemura A, Ono M, Tei S, Takahashi H, Aso T, Fukuyama H, Murai T. Altered brain response to others' pain in major depressive disorder. J Affect Disord 2014;165:170-5.
42. Girdler SS, Straneva PA, Light KC, Pedersen CA, Morrow AL. Allopregnanolone levels and reactivity to mental stress in premenstrual dysphoric disorder. Biol Psychiatry 2001;49:788-97.
43. Klatzkin RR, Bunevicius A, Forneris CA, Girdler S. Menstrual mood disorders are associated with blunted sympathetic reactivity to stress. J Psychosom Res 2014;76:46-55.
44. Dubol M, Epperson CN, Lanzenberger R, Sundström-Poromaa I, Comasco E. Neuroimaging premenstrual dysphoric disorder: A systematic and critical review. Front Neuroendocrinol 2020;57:100838.
45. Okon-Singer H, Hendler T, Pessoa L, Shackman AJ. The neurobiology of emotion-cognition interactions: fundamental questions and strategies for future research. Front Hum Neurosci 2015;9:58.
46. Vriend C, Raijmakers P, Veltman DJ, van Dijk KD, van der Werf YD, Foncke EM, Smit JH, Berendse HW, van den Heuvel OA. Depressive symptoms in Parkinson's disease are related to reduced 123IFP-CIT binding in the caudate nucleus. J Neurol Neurosurg Psychiatry 2014;85:159-64.
47. Pu R, Wu Z, Yu W, He H, Zhou Z, Wang Z, Zhong J. The association of myelination in the internal capsule with iron deposition in the basal ganglia in macaques: a magnetic resonance imaging study. Quant Imaging Med Surg 2020;10:1526-39.
48. Lu Y, Liang H, Han D, Mo Y, Li Z, Cheng Y, Xu X, Shen Z, Tan C, Zhao W, Zhu Y, Sun X. The volumetric and shape changes of the putamen and thalamus in first episode, untreated major depressive disorder. Neuroimage Clin 2016;11:658-66.
49. Liao H, Yi J, Cai S, Shen Q, Liu Q, Zhang L, Li J, Mao Z, Wang T, Zi Y, Wang M, Liu S, Liu J, Wang C, Zhu X, Tan C. Changes in Degree Centrality of Network Nodes in Different Frequency Bands in Parkinson's Disease With Depression and Without Depression. Front Neurosci 2021;15:638554.
50. Zhang Y, Zhu C, Chen H, Duan X, Lu F, Li M, Liu F, Ma X, Wang Y, Zeng L, Zhang W, Chen H. Frequency-dependent alterations in the amplitude of low-frequency fluctuations in social anxiety disorder. J Affect Disord 2015;174:329-35.
51. Etkin A, Egner T, Kalisch R. Emotional processing in anterior cingulate and medial prefrontal cortex. Trends Cogn Sci 2011;15:85-93.
52. Dixon ML, Thiruchselvam R, Todd R, Christoff K. Emotion and the prefrontal cortex: An integrative review.

Psychol Bull 2017;143:1033-81.
53. Betzel RF, Bassett DS. Specificity and robustness of long-distance connections in weighted, interareal connectomes. Proc Natl Acad Sci U S A 2018;115:E4880-9.
54. Gingnell M, Bannbers E, Wikström J, Fredrikson M, Sundström-Poromaa I. Premenstrual dysphoric disorder and prefrontal reactivity during anticipation of emotional stimuli. Eur Neuropsychopharmacol 2013;23:1474-83.
55. Grahn JA, Parkinson JA, Owen AM. The cognitive functions of the caudate nucleus. Prog Neurobiol 2008;86:141-55.
56. Aouizerate B, Cuny E, Martin-Guehl C, Guehl D, Amieva H, Benazzouz A, Fabrigoule C, Allard M, Rougier A, Bioulac B, Tignol J, Burbaud P. Deep brain stimulation of the ventral caudate nucleus in the treatment of obsessive-compulsive disorder and major depression. Case report. J Neurosurg 2004;101:682-6.
57. Liu B, Wang G, Gao D, Gao F, Zhao B, Qiao M, Yang H, Yu Y, Ren F, Yang P, Chen W, Rae CD. Alterations of GABA and glutamate-glutamine levels in premenstrual dysphoric disorder: a 3T proton magnetic resonance spectroscopy study. Psychiatry Res 2015;231:64-70.
58. Rzepa E, McCabe C. Anhedonia and depression severity dissociated by dmPFC resting-state functional connectivity in adolescents. J Psychopharmacol 2018;32:1067-74.
59. Miller AH, Jones JF, Drake DF, Tian H, Unger ER, Pagnoni G. Decreased basal ganglia activation in subjects with chronic fatigue syndrome: association with symptoms of fatigue. PLoS One 2014;9:e98156.
60. Capuron L, Pagnoni G, Drake DF, Woolwine BJ, Spivey JR, Crowe RJ, Votaw JR, Goodman MM, Miller AH. Dopaminergic mechanisms of reduced basal ganglia responses to hedonic reward during interferon alfa administration. Arch Gen Psychiatry 2012;69:1044-53.
61. Dreher JC, Schmidt PJ, Kohn P, Furman D, Rubinow D, Berman KF. Menstrual cycle phase modulates reward-related neural function in women. Proc Natl Acad Sci U S A 2007;104:2465-70.
62. De Bondt T, Smeets D, Pullens P, Van Hecke W, Jacquemyn Y, Parizel PM. Stability of resting state networks in the female brain during hormonal changes and their relation to premenstrual symptoms. Brain Res 2015;1624:275-85.
63. Beltz AM, Moser JS. Ovarian hormones: a long overlooked but critical contributor to cognitive brain structures and function. Ann N Y Acad Sci 2020;1464:156-80.
64. Taxier LR, Gross KS, Frick KM. Oestradiol as a neuromodulator of learning and memory. Nat Rev Neurosci 2020;21:535-50.
65. Kong D, Liu R, Song L, Zheng J, Zhang J, Chen W. Altered Long- and Short-Range Functional Connectivity Density in Healthy Subjects After Sleep Deprivations. Front Neurol 2018;9:546.
66. Del Felice A, Formaggio E, Storti SF, Fiaschi A, Manganotti P. The gating role of the thalamus to protect sleep: an f-MRI report. Sleep Med 2012;13:447-9.

Cite this article as: Liu C, Duan G, Zhang S, Wei Y, Liang L, Geng B, Piao R, Xu K, Li P, Zeng X, Deng D, Liu P. Altered functional connectivity density and structural covariance networks in women with premenstrual syndrome. Quant Imaging Med Surg 2023;13(2):835-851. doi: 10.21037/qims-22-506

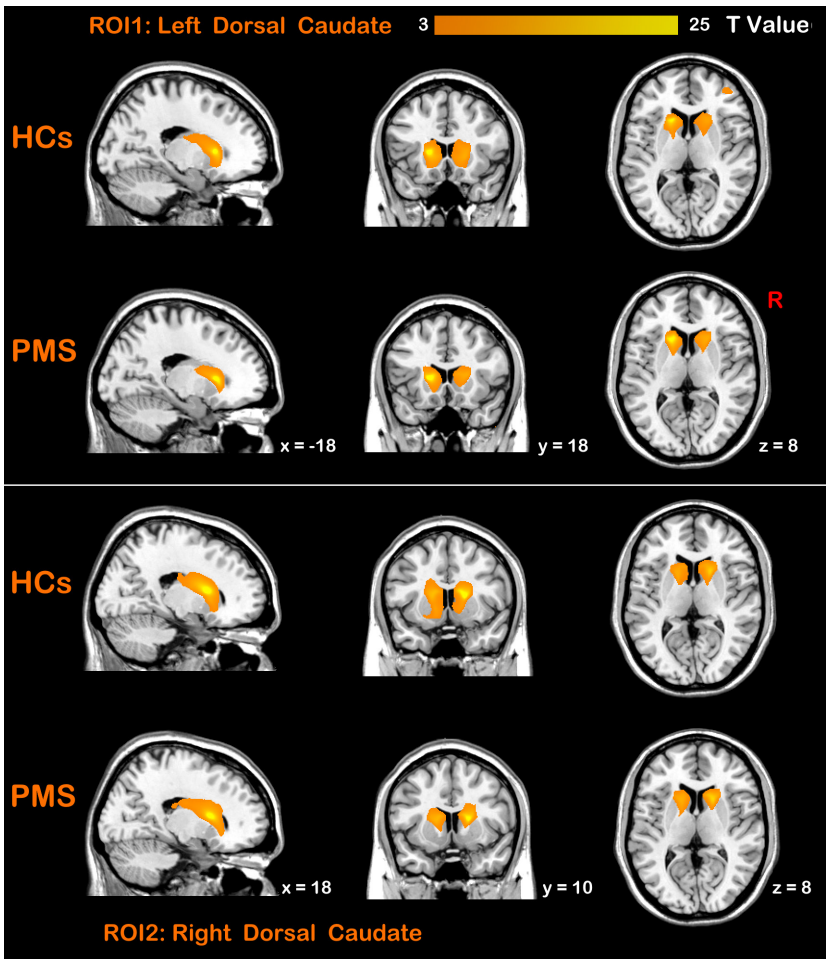

Figure S1 Bilateral dorsal caudate subregions (ROI 1–2)-based structural covariance patterns in both PMS patients and HCs. ROI, region of interest; PMS, premenstrual syndrome; HCs, healthy controls; R, right.

https://dx.doi.org/10.21037/qims-22-506

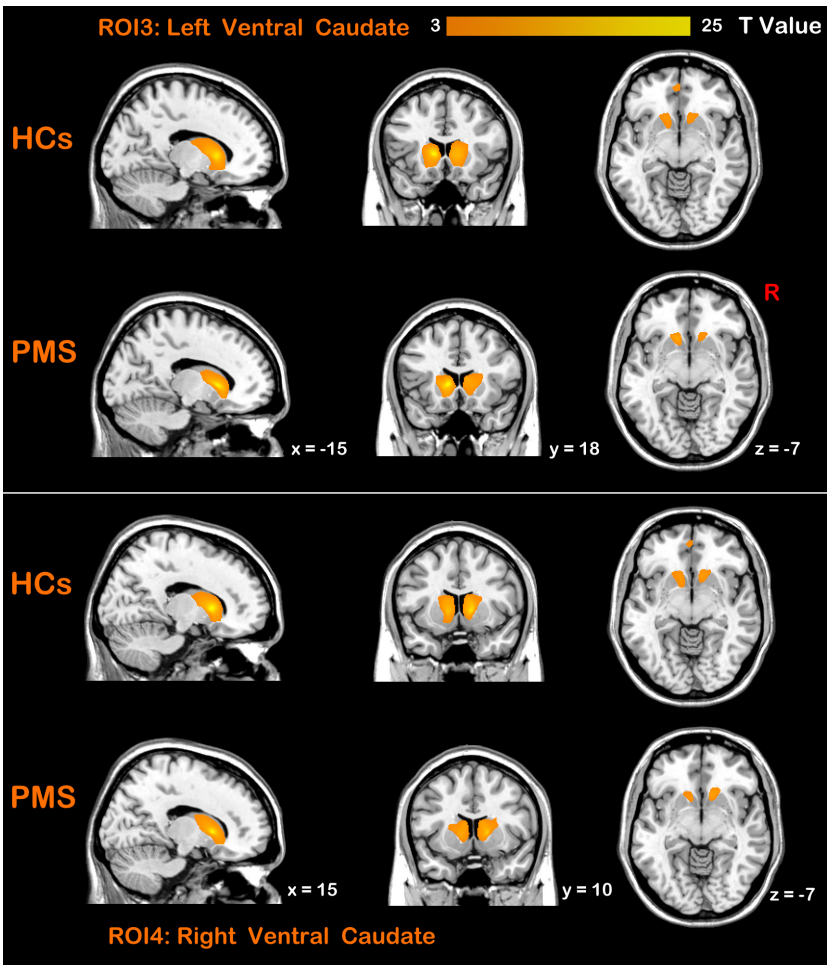

Figure S2 Bilateral ventral caudate subregions (ROI 3–4)-based structural covariance patterns in both PMS patients and HCs. ROI, region of interest; PMS, premenstrual syndrome; HCs, healthy controls; R, right.

https://dx.doi.org/10.21037/qims-22-506

Table S1 Main effect of the group on LFCD and LRFCD by two-way ANOVA

Item	Brain regions	L/R	BA	MNI coordinates (mm)			F value	Cluster P value
				x	y	z		
LFCD	MCC	L	23	–6	–18	42	13.47	<0.05
LRFCD	PreCG	L	6	–39	6	39	11.98	<0.05

L, left; R, right; BA, Brodmann area; MNI, Montreal Neurological Institute; LFCD, local functional connectivity density; LRFCD, long-range functional connectivity density; MCC, middle cingulate cortex; PreCG, precentral gyrus; ANOVA, analysis of variance.

Table S2 Interaction effects between the group and frequency band by two-way ANOVA

Item	Brain regions	L/R	BA	MNI coordinates (mm)			F value	Cluster P value
				x	y	z		
LFCD								
Cluster 1	Caudate	L	–	–18	–15	24	12.79	<0.05
	Putamen	L	–	–24	–3	6	11.59	
	Pallidum	L	–	–24	–6	3	10.37	
	Thalamus	L	–	–21	–12	6	11.66	
LRFCD	OFC	R	11	30	63	0	19.30	<0.05

L, left; R, right; BA, Brodmann area; MNI, Montreal Neurological Institute; LFCD, local functional connectivity density; LRFCD, long-range functional connectivity density; OFC, orbitofrontal cortex; ANOVA, analysis of variance.

https://dx.doi.org/10.21037/qims-22-506